ADVANCED FUNCTIONAL MATERIALS

FULL PAPER

DOI: 10.1002/adfm.200500830

Carbide-Derived Carbons: Effect of Pore Size on Hydrogen Uptake and Heat of Adsorption**

By *Gleb Yushin*, *Ranjan Dash*, *Jacek Jagiello*, *John E. Fischer*, and *Yury Gogotsi**

Cryoadsorption is a promising method of enhancing gravimetric and volumetric onboard H_2 storage capacity for future transportation needs. Inexpensive carbide-derived carbons (CDCs), produced by chlorination of metal carbides, have up to 80 % open-pore volume with tunable pore size and specific surface area (SSA). Tuning the carbon structure and pore size with high sensitivity by using different starting carbides and chlorination temperatures allows rational design of carbon materials with enhanced C–H_2 interaction and thus increased H_2 storage capacity. A systematic experimental investigation of a large number of CDCs with controlled pore size distributions and SSAs shows how smaller pores increase both the heat of adsorption and the total volume of adsorbed H_2. It has been demonstrated that increasing the average heat of H_2 adsorption above 6.6 kJ mol^{-1} substantially enhances H_2 uptake at 1 atm (1 atm = 101 325 Pa) and –196 °C. The heats of adsorption up to 11 kJ mol^{-1} exceed values reported for metal–organic framework compounds and carbon nanotubes.

1. Introduction

H_2 storage in solids occurs by physisorption, chemisorption, and/or chemical reaction. Carbon-based materials have received considerable attention in the context of physisorption.[1] Sorption processes require porous materials with a large number of sorption sites per unit mass or volume of an adsorbent, in other words materials with high specific surface area (SSA) (either gravimetric or volumetric) accessible to the sorbate. Many carbon structures with high SSA are known: activated carbon, exfoliated graphite, fullerenes, carbon nanotubes (CNTs), nanofibers, and so forth. Investigations of H_2 storage in carbons as a function of SSA have been reported over the last three decades, and activated carbons with SSAs up to ca. 3000 m^2 g^{-1} have been produced.[2]

Intuitively, H_2 adsorption on carbons comprised of graphene sheets should depend linearly on the SSA, and the concept has been generalized to CNTs and to carbons lacking graphitic short-range order.[1,3,4] The amount of reversibly adsorbed H_2 on nanostructured graphitic carbon at –196 °C correlates to a SSA for a large number of materials ranging from nanotubes to activated carbon (Fig. 1). It amounts to ca. 1.1 wt % per 1000 m^2 g^{-1} of SSA (Fig. 1).[3] Since the SSA for two sides of a graphene sheet is 2620[5]–2965 m^2 g^{-1},[6] ca. 3 wt % appears to be the limit for low-temperature, ambient-pressure storage. This, along with low measured H_2 uptake at room temperature[3,7] and numerous errors in the measurements of H_2 uptake by carbon nanostructures, has led to loss of confidence in carbon's potential for H_2 storage.

This pessimism may have been premature. The data in Figure 1 were obtained from samples with different surface chem-

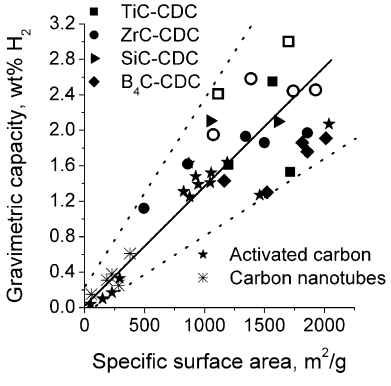

Figure 1. H_2 uptake at 1 atm (1 atm = 101 325 Pa) and –196 °C for various porous carbon materials as a function of Brunauer–Emmett–Teller (BET) SSA. Solid symbols stand for as-produced and hollow for H_2-treated CDCs. H_2 storage capacity generally increases with SSA. The solid line shows a linear fit with a slope of ca. 1.1 wt % per 1000 m^2 g^{-1}. Carbon nanomaterials with similar surface areas show large variations in H_2 storage capacity.

[*] Prof. Y. Gogotsi, Prof. G. Yushin, R. Dash
Department of Materials Science and Engineering and
A. J. Drexel Nanotechnology Institute, Drexel University
Philadelphia, PA 19104 (USA)
E-mail: gogotsi@drexel.edu
J. Jagiello
Quantachrome Instruments
1900 Corporate Dr., Boynton Beach, FL 33426 (USA)
Prof. J. E. Fischer
Department of Materials Science and Engineering
University of Pennsylvania, Philadelphia, PA 19104 (USA)

[**] This work was supported by the US Department of Energy under grant No. DE-FC36-04GO14282 via the University of Pennsylvania. HRTEM studies were performed in Penn Regional Nanotechnology Facility, University of Pennsylvania. Additional material characterization was performed in Drexel University Centralized Materials Characterization Facility. We thank G. Laudisio and T. Yildirim for helpful discussions. Activated carbon was kindly provided by Dr. Richard Chanine, University of Quebec. SiC was provided by Superior Graphite Co. (USA).

ADVANCED FUNCTIONAL MATERIALS

istry, structure, and graphene curvature. While these differences are generally ignored,[3] it is well known in adsorption science that parameters other than the SSA may strongly influence the sorbent properties.[8] Figure 1 supports this statement by demonstrating large variations in H_2 storage capacities in samples with similar SSA. Clearly, in order to maximize the H_2 sorption at the desired temperature (T) and pressure (P) one needs not only to maximize the number of adsorption sites per unit mass and volume of the solid (which could indeed be proportional to SSA) but also tune the H_2–solid interaction energy that would allow more sorption sites to adsorb H_2 molecules. Optimizing the adsorbent structure for increased adsorption per SSA is at least as important as maximizing the SSA. If all the pores in high SSA materials were filled with adsorbed H_2, a very high gravimetric H_2 storage would be possible. Figure 2 shows the maximum possible H_2 uptake as a function of pore volume calculated for complete pore filling by either solid or

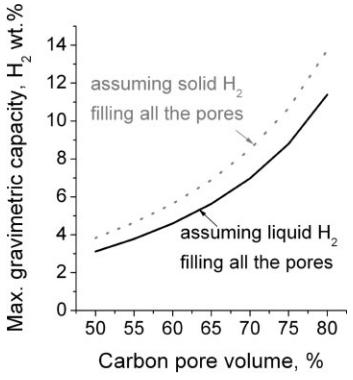

Figure 2. Maximum possible H_2 uptake for porous carbon materials as a function of carbon porosity. Pores are assumed to be fully filled either with solid (density ≈ 0.088 g cm^{-3}) or liquid (density ≈ 0.071 g cm^{-3}) H_2 condensed on the carbon surface.

liquid H_2. Porous carbons with pores occupying 78 % or more of the volume (pore volume ca. 1.6 cm^3 g^{-1}) could potentially exceed the long-term target of the US Department of Energy (DOE) of 10 wt % if the H_2–C interaction were optimized. This observation justifies further studies on carbon materials to design efficient H_2 sorbents.

Gas adsorption takes place when the interaction energy between an adsorbate molecule and adsorbent is equal to the work needed to bring a free molecule to the adsorbed state at a given temperature. Most theories approximate the adsorbed state as the saturated pressure (P_0) state. At this approximation, for a given T and P one can calculate the work needed for an average molecule to be adsorbed. As such, one can either determine at what P most molecules get adsorbed when the interaction energy and T are known, or estimate the interaction energy for gas molecules to be adsorbed at the desired P and T. Surprisingly, little experimental research has been carried out on the parameters that influence the H_2–sorbent interaction potential. There remains a lack of understanding of the relation between the surface chemistry, microstructure, and porosity of carbon and its interaction with H_2 molecules. There have been only a few systematic studies, mostly theoretical, of the effects of pore size on the carbon–H_2 interaction.[9–13] Very recent calculations[13] show that the heat of adsorption of H_2 on an "ideal" adsorbent should be ca. 15 kJ mol^{-1}, if both the delivery and storage is to occur at room temperature. This value is considerably higher than the average heat of adsorption of H_2 on activated carbons and CNTs (5–6.5 kJ mol^{-1}), as well as on metal–organic frameworks (MOFs, 0–7 kJ mol^{-1}).

We recently reported[14] the effect of pore size on the H_2 sorption and demonstrated an increased H_2 uptake in materials with smaller pores. In particular, we showed that a pore width of ca. 0.6 nm could be the optimum for H_2 storage. Here we present a detailed analysis of the mechanisms of H_2 storage to provide guidance for future material development.

The sorption experiments were performed mainly on porous carbons prepared by high-temperature chlorination of carbides, referred to as carbide-derived carbons (CDCs).[15] Our choice of this class of porous carbons was determined by the ability to finely tune the pore size distribution (PSD) by controlling the parameters of the synthesis process.[15,16] In addition, CDCs are known to have a high SSA and tunable pore volume, and many of the precursor carbides are inexpensive.[15] The discussed properties of CDC make it not only a good material for fundamental studies, but also a promising candidate for gas-storage applications.

2. Results and Discussion

2.1. Structure and Porosity

Selective removal of metals from metal carbides results in the formation of porous carbon with a density lower than that of graphite. In the 1960s, CDCs were produced as a byproduct of metal chloride synthesis according to the reaction

$$MeC + x/2\ Cl_2 = MeCl_x + C \quad (1)$$

where Me is a carbide-forming metal. At that time, CDC was considered to be an undesirable byproduct and it was periodically burned in the reactor to increase the chloride production rate.[15]

The pore size of CDCs is influenced by the spatial distribution of carbon atoms in the precursor carbide, the synthesis temperature, the size of the chloride molecules, the presence of catalytic particles, and the effect of optional post-treatments, such as purification or activation.[15] Figure 3 shows the PSDs of CDCs derived from TiC, ZrC, B_4C, and SiC chlorinated at different temperatures. A low temperature (< 600 °C) generally results in very uniform pore size. The PSDs are narrower than those measured from single-walled CNTs (SWCNTs) and typical activated carbons and are comparable to zeolites. Increasing the synthesis temperature leads to pore enlargement and broader PSDs. Some samples were annealed in H_2 for 2 h at 600 °C to remove residual chlorine trapped in nanopores during synthesis. This procedure resulted in increased SSA and micropore volume accessible to argon. Opening of small pores

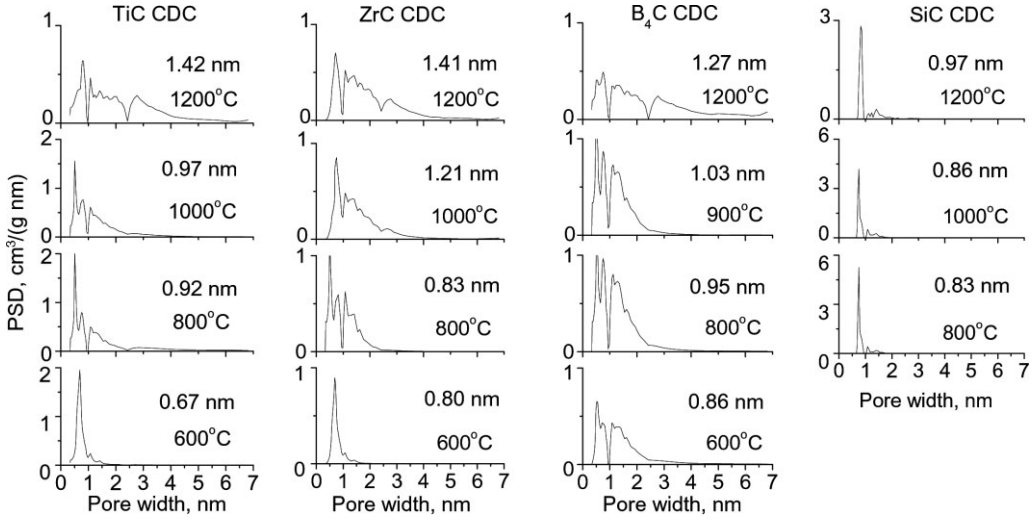

Figure 3. Pore size distributions of the CDCs as a function of synthesis temperature calculated using nonlocal density functional theory (NLDFT). The minima at about 1 and 2.5 nm are artifacts of the DFT method. Synthesis temperature and average pore size are indicated in each graph.

and shifting the PSD to smaller values was also generally observed (data not shown).

A gradual evolution of CDC structure as the chlorination temperature increases was revealed using Raman spectroscopy, X-ray diffraction (XRD),[17–20] and transmission electron microscopy (TEM; Fig. 4). At low synthesis temperatures, CDCs consist of amorphous carbon with no distinguishable graphite fringes (Fig. 4a). As the synthesis temperature increases to about 800 °C (Fig. 4b), most CDCs (including those obtained from B_4C, TiC, and ZrC) reorganize into highly curved single graphene sheets (fullerene-like structures). At even higher temperatures, curved thin graphite ribbons with an interplanar distance of ca. 0.34 nm appear in the TEM images (Fig. 4c and d). Amorphous carbon is still present in these samples but in a considerably smaller quantity. In contrast to other CDCs, SiC derived CDCs remain amorphous up to 1200 °C.[21] Changes in CDC microstructure are inherently connected to changes in pore structure. Amorphous structures formed at lower temperatures are clearly associated with uniform and relatively small pores, whereas graphitic ribbon network structures formed at higher synthesis temperatures are linked to less uniform and generally larger pores (compare Figs. 3 and 4).

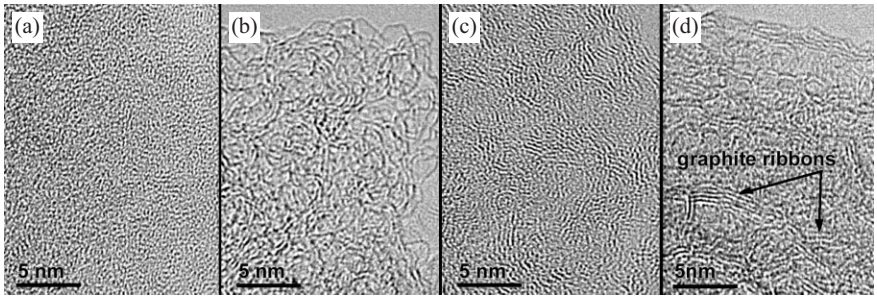

Figure 4. TEM images of the CDCs synthesized from TiC at 400 (a), 800 (b), 1000 (c), and 1200 °C (d). Graduate structure evolution is observed as the chlorination temperature increases.

2.2. H_2 Sorption

Plotting the H_2 adsorption capacity of carbon surfaces as a function of the average pore size[14] clearly defines the trend of increasing storage with decreasing pore size. However, the experimental data are scattered because materials with different PSDs may have the same average pore size. In order to separate the contributions of larger and smaller pores, we plotted the H_2 uptake as a function of volume and SSA of pores below and above 1 nm (Fig. 5) separately and found a linear increase for pores smaller than 1 nm (Fig. 5a and b). Small deviations from linearity occur in materials that have a high additional SSA associated with pores larger than 1 nm. A large volume of larger pores may contribute significantly at 1 atm (1 atm = 101 325 Pa), in spite of their lower efficiency. In a similar plot for H_2 uptake at 0.1 atm, where a stronger interaction is needed for H_2 adsorption and therefore the contribution from large pores should be further diminished, these deviations tend to disappear (Fig. 6). In contrast, we find no correlation between the total H_2 uptake and volume and the SSA of larger pores (Fig. 5c and d). This supports our previous results[14] and also explains the origin of the large data scattering observed in Figure 1. Comparison of the observed uptake and the maximum amount of H_2 able to fill all the pores less than 1 nm (solid line in Fig. 5a), suggests that, independent of other parameters, smaller pores are nearly completely filled with adsorbed H_2 at –196 °C and 1 atm.

Smaller pores are clearly more efficient in H_2 sorption due to a stronger interaction with the H_2 molecules. The total interaction between the adsorbate molecule and a solid is greater if the molecule can interact with a larger number of surface atoms, as happens in small curved pores (Fig. 4a and b) or narrow slit pores. When

ADVANCED FUNCTIONAL MATERIALS

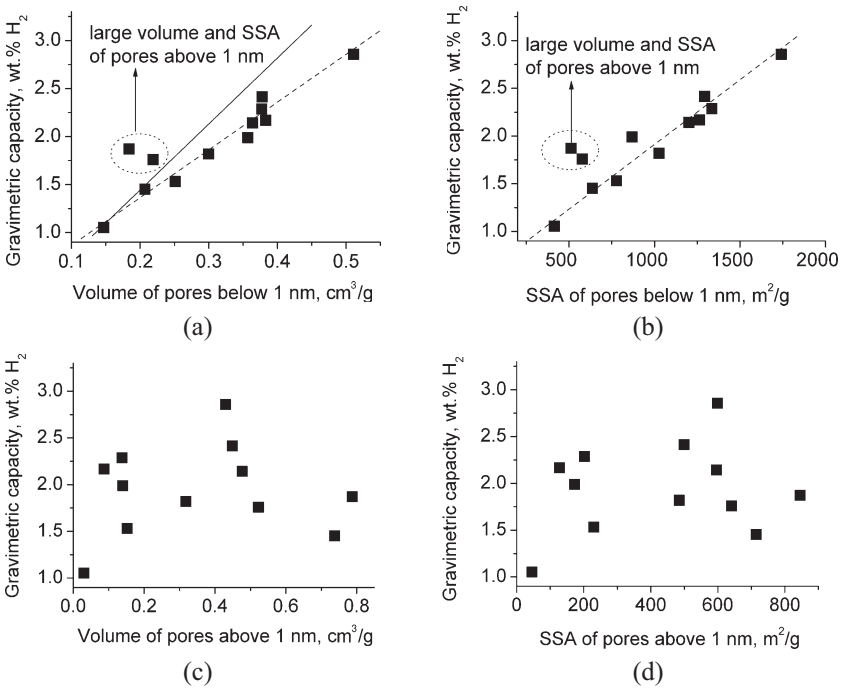

Figure 5. H_2 uptake at 1 atm and –196 °C versus volume and SSA of pores below (a,b) and above (c,d) 1 nm. While a larger volume of smaller pores was seen to increase H_2 storage almost linearly, no correlations were found between the volume or surface area of larger pores and H_2 capacity of CDCs. Solid line in (a) corresponds to the maximum amount of H_2 that could be stored in pores less than 1 nm, assuming H_2 density = 0.071 g cm^{-3} (liquid H_2 density). The SSA was calculated using the NLDFT method.

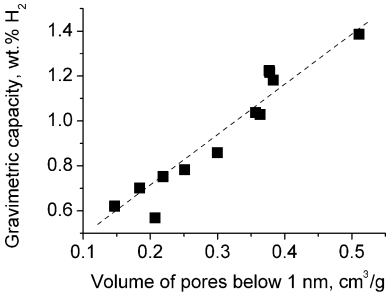

Figure 6. H_2 uptake at 0.1 atm and –196 °C as a function of the volume of pores below 1 nm.

a molecule is located in a slit pore, the sorbate–sorbent interaction potentials from both sides of the pore wall overlap to a degree determined by the pore width. A good illustration is the known decrease of the threshold pressure for Ar adsorption with decreasing pore size.[8] While such an influence has rarely been discussed in papers on H_2 storage, the phenomenon is well known. In fact, nearly all gas-sorption theories employed in the software supplied with commercial instruments to derive PSDs from sorption isotherms take it into account. One should always expect a stronger interaction if the molecule is placed inside a small pore, as compared to a larger one, or to an exterior solid surface, such as the basal plane of graphite or the outer surface of a single nanotube.

The opening of additional small pores in CDCs by annealing in H_2 led to a higher H_2 sorption capacity, with values up to 336 cm^3 g^{-1} (3.0 wt %), as shown in Figure 7. H_2 treatment increased the storage by as much as 75 % for some materials. This clearly shows the effect of pore accessibility on the sorption of H_2 by porous carbons. The superior performance of CDCs compared to that of SWCNTs, multiwalled CNTs, and MOF-5 at ambient pressure has been shown in the literature.[14] CDCs can store over 20 % more H_2 than advanced MOFs (ca. 1.3 wt % in MOF-5;[14] ca. 1.4 wt % in $Cu_3(BTC)_2(H_2O)_3$;[22] ca. 2 wt % in $[Co_3(bpdc)_3bpy]\cdot 4\,DMF\cdot H_2O$;[23] ca. 2.48 wt % in MOF-505[24,25]) and >several times that of CNTs (< 0.9 wt %[14]). They also outperform the benchmark activated carbon (Fig. 7) and low-temperature metal hydrides.[26] Since SWCNTs and most MOFs have a SSA comparable to or greater than CDCs, the observed uptake variations could be explained by the presence of a narrow distribution of small pores in CDCs. However, the strength of interaction between H_2 and the sorbent may be another important factor.

The heat of H_2 adsorption on CDCs calculated for selected materials characterizes the interaction between H_2 and carbon. Stronger interactions should result in a higher H_2 coverage of the sorbent surface, if H_2 sorption sites are available. Figure 8 demonstrates the experimentally observed increase in H_2 uptake at 1 atm and –196 °C per surface area as the integrated average heat of adsorption grows, in agreement with theoretical calculations.[13] For H_2 adsorption at room temperature, a larger heat of adsorption is required due to the higher kinetic energy of ca. 3.6 kJ mol^{-1} and the larger work needed to adsorb an average molecule. So far, CDC heats of H_2 adsorption noticeably exceed those of MOFs, CNTs, and activated carbons (Fig. 9). Selected sorption sites in the CDC demonstrated H_2 heat of adsorptions in excess of 8 kJ mol^{-1}. To the best of our knowledge,

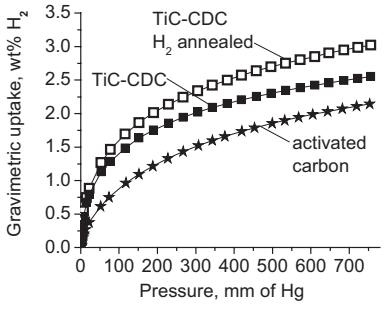

Figure 7. H_2 sorption isotherms at –196 °C. CDCs produced from TiC at 800 °C before and after 2 h H_2 annealing at 600 °C. Data for the benchmark activated carbon are shown for comparison.

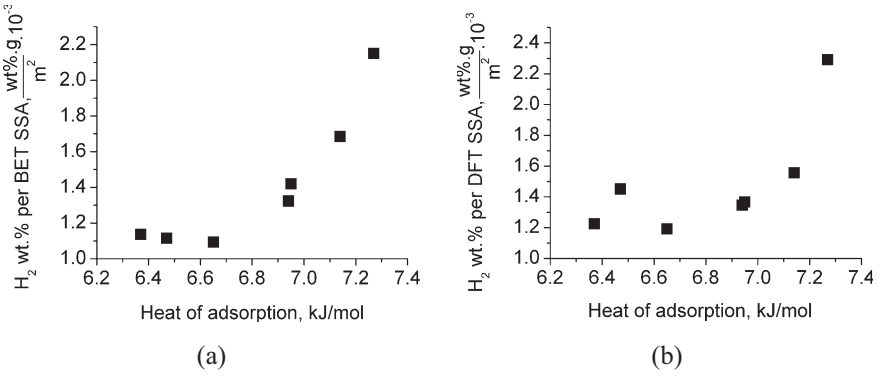

Figure 8. H_2 uptake at 1 atm and –196 °C per a) BET and b) DFT surface area versus the integrated average heat of adsorption.

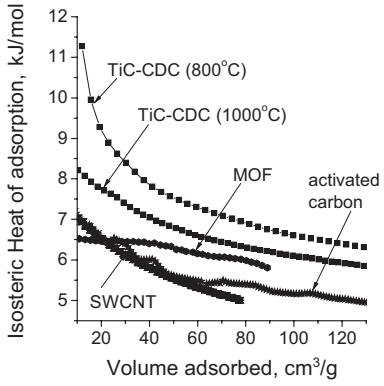

Figure 9. H_2 heat of adsorption. CDC produced from TiC at 800 °C and 1000 °C compared to the benchmark activated carbon, MOF ($Cu_3(BTC)_2(H_2O)_3$) [22], and SWCNT.

such high experimental values have not been reported for carbon-based adsorbents before.[27] CDC with smaller pores systematically shows a considerably stronger C–H_2 interaction.

While we observed a correlation between the H_2 adsorption and pore size in CDCs, we cannot exclude the possibility that other parameters of carbon microstructure, such as pore shape, degree of disorder, or internal surface chemistry, may influence sorption properties as well. For a given pore size (minimum pore dimension), cylindrical and spherical pores may result in a different total sorbate–sorbent interaction compared to slit-shaped pores. In addition, different sorption sites may exhibit variations in interaction potentials due to differences in the arrangement of neighboring atoms or directionality and type of bonding. It is well known that graphite orientation strongly influences its ability to adsorb electrolyte ions on the surface: edge planes of graphite exhibit up to 70 times higher specific capacitance compared to the basal planes under identical conditions.[28] Gas sorbates may exhibit similar site or orientation dependence. In addition, surface functionalities, impurities, or dopants are more likely to be attached to the edges of the graphitic planes. Greater disorder (higher percentage of carbon edge atoms) may result in a stronger influence of carbon surface chemistry on H_2 sorption properties. While some carbon nanomaterials such as CNTs mostly have basal planes of graphite exposed to a sorbate gas, highly porous activated carbons and CDCs exhibit a high percentage of edge plane atoms available for H_2 sorption. The presence of trace-metal atoms in CDC of up to 0.5 at % could also potentially play a role in H_2 uptake and heat of adsorption, as theoretically predicted and demonstrated in several recent publications.[29,30]

In general, our results are in fairly good agreement with literature data for activated carbons.[3,31] Porous carbons with a large volume of small pores show a high uptake of H_2, while carbons with a high SSA, but larger pores demonstrate a moderate H_2 capacity. On the other hand, differences in chemical composition and structure between CDC and activated carbons may cause some differences in the H_2 heat of adsorption and storage capacity.

While high gravimetric H_2 uptake can be achieved in CDC, it is important to underscore CDCs principal advantage in volumetric uptake of H_2 compared to all other carbons. All powdered, pelletized, or pressed activated carbons contain 40 % or more of macropores as space between micrometer-sized particles, which cannot contribute to storage by physisorption. Conversely, CDCs produced from bulk ceramics[32] have no macroporosity, thus, almost 100 % of the pore volume contributes to H_2 storage. Volumetric capacity enhancements of about 40 % can be realized compared to other carbons with the same micropore size/volume. Thus, gas tanks filled with densely packed CDC plates or bricks may provide the maximum volumetric storage of H_2. The 0.8 g cm^{-3} density of the bulk CDC with 3 wt % gravimetric capacity translates into 24 kg m^{-3} volumetric capacity.

3. Conclusions

Optimized CDCs have the potential to meet the needs of a H_2 economy. CDCs with gravimetric H_2 storage density up to 3.0 wt % and volumetric density up to 24 kg m^{-3} at 1 atm pressure and –196 °C, have demonstrated a higher volumetric and gravimetric storage capacity compared to benchmark activated carbon, MOFs, SWCNTs, MWCNTs, and low-temperature metal hydrides. These values are believed to be due to smaller average pore size and higher average heat of H_2 adsorption in selected CDC samples. Considering that less than half the total CDC pore volume accessible to argon is currently used by H_2 at ambient pressure, there is great potential for increased storage density by increasing pressure or by further tuning the PSDs. While small pores (1 nm or below) are efficient for H_2 sorption, pores above 1 nm do not contribute much to the storage of H_2 at ambient pressure and liquid-nitrogen temperature.

4. Experimental

Material Synthesis: We synthesized CDCs from commercially available powders of B_4C [17], ZrC [18], TiC [20], and SiC [19] at various

ADVANCED FUNCTIONAL MATERIALS

temperatures in the 400–1200 °C range. TiC, ZrC, and B_4C with an average particle size of ca. 2–4 μm were obtained from Alfa Aesar, while β-SiC powder with an average particle size of ca. 2 μm was obtained from Superior Graphite. Chlorination experiments were performed on as-received samples using high-purity chlorine (BOC Gases, UHV grade) and argon (BOC Gases, UHV grade) as reactive and purging gases, respectively. For CDC synthesis, selected carbide powder was placed onto a quartz sample holder and loaded into the hot zone of a horizontal quartz tube furnace. The tube was Ar purged for 30 min before heating at a rate of ca. 30 °C min^{-1} to the desired temperature. Once the desired temperature was reached and stabilized, the Ar flow was stopped and a 3 h chlorination began in Cl_2 flowing at a rate of 10 sccm. After completion of the chlorination process, the samples were cooled down under a flow of Ar to remove residual metal chlorides from the pores, and taken out for further analyses. In order to avoid a backstream of air the exhaust tube was connected to a bubbler filled with sulfuric acid. A detailed description of the chlorination apparatus used in this study can be found in the literature [15].

A sample of IRH33 activated carbon from the Institute for Hydrogen Research of the University of Quebec was used as a benchmark material. It was tested in a Round Robin organized by the US DOE and is similar to AX-21 [27].

Characterization and H_2 Sorption Measurements: The structure of the CDC was investigated using high-resolution transmission electron microscopy (HRTEM). The TEM samples were prepared through using a 2 min sonication of the CDC powder in isopropyl alcohol and deposition on the lacey-carbon-coated copper grid (200 mesh). A field-emission transmission electron microscope (JEOL 2010F, Japan) with an imaging filter (Gatan GIF) was used at 200 kV.

Porosity and H_2 sorption properties of CDC were studied using an automated micropore gas analyzer Autosorb-1 (Quantachrome Instruments, USA). The Ar sorption isotherms collected at liquid-nitrogen temperature (–196 °C) were analyzed using the Brunauer–Emmett–Teller (BET) equation and nonlocal density functional theory (NLDFT) [33–38] to reveal the SSA and PSDs of CDC. Quantachrome's data reduction software Autosorb v.1.27 [31] was employed for these calculations. The weighted pore size of the CDC was calculated from the PSD using numerical integration of:

$$\frac{\int_{0\text{nm}}^{7\text{nm}} wV\,\mathrm{d}w}{\int_{0\text{nm}}^{7\text{nm}} V\,\mathrm{d}w} \qquad (2)$$

where w is the pore width and V is the differential pore volume. H_2 sorption measurements were performed at –196 °C and selectively at liquid-argon temperature (–186 °C). The gravimetric storage density of H_2 (wt %) was defined as $(\rho_{\text{Hydrogen}} \cdot \nu_{\text{Hydrogen}} \cdot 100)$, where ρ_{Hydrogen} is the H_2 density; ν_{Hydrogen} is the volume of H_2 adsorbed at –196 °C and 1 atm in a unit mass of CDC. This definition is currently very common in publications on H_2 sorption, but it gives slightly higher values compared to the one where the mass of adsorbed gas is normalized by the total mass of the adsorbent/adsorbate system. The density of bulk CDC was defined as the mass to geometrical volume ratio. To reveal the influence of pore size on the H_2–carbon interaction, H_2 sorption measurements on a series of CDC samples at both cryogenic temperatures were analyzed using the Clausius–Clapeyron equation [8,37,38]:

$$Q_{\text{st}} = \frac{R.\ln\left(P_{87.4}/P_{77.3}\right)}{\left(1/77.3 - 1/87.4\right)} \qquad (3)$$

where Q_{st} is the heat of adsorption, R is a real gas constant; $P_{87.4}$ and $P_{77.3}$ are H_2 pressures obtained from a B-Spline fitted H_2 isotherm at liquid-argon and liquid-nitrogen temperatures, respectively.

Received: November 22, 2005
Revised: April 15, 2006

[1] M. G. Nijkamp, J. E. M. J. Raaymakers, A. J. van Dillen, K. P. de Jong, *Appl. Phys. A* **2001**, *72*, 619.
[2] D. Lozano-Castello, D. Cazorla-Amoros, A. Linares-Solano, *Energy Fuels* **2002**, *16*, 1321.
[3] L. Schlapbach, A. Zuttel, *Nature* **2001**, *414*, 353.
[4] A. Zuttel, P. Sudan, P. Mauron, T. Kiyobayashi, C. Emmenegger, L. Schlapbach, *Int. J. Hydrogen Energy* **2002**, *27*, 203.
[5] K. R. Matranga, A. L. Myers, E. D. Glandt, *Chem. Eng. Sci.* **1992**, *47*, 1569.
[6] H. K. Chae, D. Y. Siberio-Pérez, J. Kim, Y. Go, M. Eddaoudi, A. J. Matzger, M. O'Keeffe, O. M. Yaghi, *Nature* **2004**, *427*, 523.
[7] H. Kajiura, S. Tsutsui, K. Kadono, M. Kakuta, M. Ata, Y. Murakami, *Appl. Phys. Lett.* **2003**, *82*, 1105.
[8] R. T. Yang, *Adsorbents: Fundamentals and Applications*, Wiley, New York **2003**.
[9] M. Rzepka, P. Lamp, M. A. de la Casa-Lillo, *J. Phys. Chem. B* **1998**, *102*, 10 894.
[10] M. A. de la Casa-Lillo, F. Lamari-Darkrim, D. Cazorla-Amoros, A. Linares-Solano, *J. Phys. Chem. B* **2002**, *106*, 10 930.
[11] Q. Y. Wang, J. K. Johnson, *J. Chem. Phys.* **1999**, *110*, 577.
[12] N. Texier-Mandoki, J. Dentzer, T. Piquero, S. Saadallah, P. David, C. Vix-Guterl, *Carbon* **2004**, *42*, 2744.
[13] S. K. Bhatia, A. L. Myers, *Langmuir* **2006**, *22*, 1688.
[14] Y. Gogotsi, R. K. Dash, G. Yushin, T. Yildirim, G. Laudisio, J. E. Fischer, *J. Am. Chem. Soc.* **2005**, *127*, 16 006.
[15] G. Yushin, Y. Gogotsi, A. Nikitin, in *Nanomaterials Handbook* (Ed: Y. Gogotsi), CRC Press, Boca Raton, FL **2005**, Ch. 8, p. 237.
[16] Y. Gogotsi, A. Nikitin, H. Ye, W. Zhou, J. E. Fischer, B. Yi, H. C. Foley, M. W. Barsoum, *Nat. Mater.* **2003**, *2*, 591.
[17] R. K. Dash, A. Nikitin, Y. Gogotsi, *Microporous Mesoporous Mater.* **2004**, *72*, 203.
[18] R. K. Dash, G. Yushin, Y. Gogotsi, *Microporous Mesoporous Mater.* **2005**, *86*, 50.
[19] D. A. Ersoy, M. J. McNallan, Y. Gogotsi, in *High Temp. Corros. Mater. Chem., Proc. Symp.*, Vol. 98–9 (Eds: P. Y. Hou, M. J. McNallan, R. Oltra, E. J. Opila, D. A. Shores), Electrochemical Society, Pennington, NJ **1998**, p. 324.
[20] R. K. Dash, J. Chmiola, G. N. Yushin, Y. Gogotsi, G. Laudisio, J. Singer, J. E. Fischer, S. Kucheyev, *Carbon* **2006**, *44*, 2489.
[21] Z. G. Cambaz, G. N. Yushin, K. L. Vyshnyakova, L. N. Pereselentseva, Y. G. Gogotsi, *J. Am. Ceram. Soc.* **2005**, *89*, 509.
[22] J. Y. Lee, J. Li, J. Jagiello, *J. Solid State Chem.* **2005**, *178*, 2527.
[23] J. Y. Lee, L. Pan, S. P. Kelly, J. Jagiello, T. J. Emge, J. Li, *Adv. Mater.* **2005**, *17*, 2703.
[24] J. L. C. Rowsell, O. M. Yaghi, *Angew. Chem. Int. Ed.* **2005**, *44*, 4670.
[25] B. Chen, N. W. Ockwig, A. R. Millward, D. S. Contreras, O. M. Yaghi, *Angew. Chem. Int. Ed.* **2005**, *44*, 4745.
[26] R. F. Service, *Science* **2004**, *305*, 958.
[27] P. Benard, R. Chahine, *Langmuir* **2001**, *17*, 1950.
[28] E. B. Yeager, J. A. Molla, S. Gupta, in *Proc. Electrochem. Soc.* Vol. 84–5 (Eds: S. Sarangapani, J. R. Akridge, B. Schumm), Electrochemical Society, Pennington, NJ **1984**, p. 123.
[29] T. Yildrim, S. Ciraci, *Phys. Rev. Lett.* **2005**, *94*, 175 501.
[30] O. Maresca, R. J.-M. Pellenq, F. Marinelli, J. Conard, *J. Chem. Phys.* **2004**, *121*, 12 548.
[31] J. Jagiello, M. Thommes, *Carbon* **2004**, *42*, 1227.
[32] D. A. Ersoy, M. J. McNallan, Y. Gogotsi, *Mater. Res. Innovations* **2001**, *5*, 55.
[33] P. I. Ravikovitch, A. V. Neimark, *Colloids Surf. A* **2001**, *187–188*, 11.
[34] S. J. Gregg, K. S. W. Sing, *Adsorption, Surface Area and Porosity*, Academic, London **1982**, p. 42.
[35] S. Brunauer, P. Emmett, E. Teller, *J. Am. Chem. Soc.* **1938**, *60*, 309.
[36] S. Lowell, J. E. Schields, *Powder Surface Area and Porosity*, Chapman and Hall, New York **1998**, p. 17.
[37] A. Magnus, R. Kieffer, *Z. Anorg. Allg. Chem.* **1929**, *179*, 215.
[38] D. M. Ruthven, *Principles of Adsorption and Adsorption Processes*, Wiley, New York **1984**.

